Generalized polarizabilities and the chiral structure of the nucleon

Thomas R. Hemmert,^a Barry R. Holstein,^b Germar Knöchlein,^c and Stefan Scherer^c *

 $^{\mathrm{a}}\mathrm{TRIUMF},$ Theory Group, 4004 Wesbrook Mall, Vancouver, British Columbia, Canada V6T $2\mathrm{A3}$

^bDepartment of Physics and Astronomy, University of Massachusetts, Amherst, Massachusetts 01003

^cInstitut für Kernphysik, Johannes Gutenberg-Universität, D-55099 Mainz, Germany

We discuss the virtual Compton scattering reaction $e^-p \rightarrow e^-p\gamma$ at low energies. We present results for the generalized polarizabilities of the nucleon obtained in heavy baryon chiral perturbation theory at $O(p^3)$.

1. INTRODUCTION

At energies below the pion-production threshold, the amplitude for Compton scattering off the nucleon may be expanded in a Taylor series in the momentum of the photon. The famous lowenergy theorem (LET) of Low [1] and Gell-Mann and Goldberger [2] makes a model-independent prediction for the expansion up to and including linear terms. The Taylor series coefficients are given in terms of the charge, mass, and magnetic moment of the target, i.e. properties of the nucleon which can entirely be determined from different experiments. The derivation of this theorem is based on gauge invariance, Lorentz covariance, crossing symmetry, and the discrete symmetries. The description of second-order terms requires two new structure constants specific to the real Compton scattering amplitude, the electric and magnetic polarizabilities $\bar{\alpha}_E$ and $\bar{\beta}_M$ (for an overview see, e.g., [3]).

The investigation of virtual Compton scattering (VCS) as tested in, e.g., the reaction $e^-p \rightarrow e^-p\gamma$, has recently attracted a lot of interest. Even though the experiments [4] will be considerably more complicated than for real Compton scattering, there is the prospect of obtaining completely new information about the structure of the nucleon which cannot be obtained from any other experiment. Like in real Compton scattering, the model-independent properties of the low-energy VCS amplitude have been identified in [5,6]. In [5] the model-dependent part beyond the LET was analyzed in terms of a multipole expansion. Keeping only terms linear in the energy of the final photon, the corresponding amplitude was parametrized in terms of ten so-called generalized polarizabilities (GPs) which are functions of the three-momentum transfer of the initial virtual photon. The number of independent GPs reduces to six, if charge-conjugation invariance is imposed [7,8].

^{*}Talk given at the 15th International Conference on Few Body Problems in Physics, Groningen, The Netherlands, 22-26 July 1997

2. KINEMATICS AND LET

Omitting the Bethe-Heitler contribution, the invariant amplitude for VCS reads

$$\mathcal{M}_{VCS} = -ie^2 \epsilon_\mu \epsilon_\nu^{\prime *} M^{\mu\nu} = -ie^2 \epsilon_\mu M^\mu = ie^2 \left(\vec{\epsilon}_T \cdot \vec{M}_T + \frac{q^2}{\omega^2} \epsilon_z M_z \right), \tag{1}$$

where $\epsilon_{\mu} = e\bar{u}\gamma_{\mu}u/q^2$ is the polarization vector of the virtual photon ($e > 0, e^2/4\pi \approx 1/137$), and where use of current conservation has been made. In the center-of-mass system, using the Coulomb gauge for the final real photon, the transverse (longitudinal) part of \mathcal{M}_{VCS} can be expressed in terms of eight (four) independent structures [6,9],

$$\vec{\epsilon}_T \cdot \vec{M}_T = \vec{\epsilon}^{\prime *} \cdot \vec{\epsilon}_T A_1 + \cdots, \quad M_z = \vec{\epsilon}^{\prime *} \cdot \hat{q} A_9 + \cdots,$$
⁽²⁾

where the functions A_i depend on three kinematical variables, $\bar{q} = |\vec{q}|, \omega' = |\vec{q}'|, z = \hat{q} \cdot \hat{q}'$.

Extending the method of Gell-Mann and Goldberger [2] to VCS, model-independent predictions for the functions A_i were obtained in [6]. For example, the result for A_1 up to second order in \bar{q} and ω' is

$$A_{1} = -\frac{1}{M} + \frac{z}{M^{2}}\bar{q} - \left(\frac{1}{8M^{3}} + \frac{r_{E}^{2}}{6M} - \frac{\kappa}{4M^{3}} - \frac{4\pi\bar{\alpha}_{E}}{e^{2}}\right)\omega'^{2} + \left(\frac{1}{8M^{3}} + \frac{r_{E}^{2}}{6M} - \frac{z^{2}}{M^{3}} + \frac{(1+\kappa)\kappa}{4M^{3}}\right)\bar{q}^{2}.$$
(3)

To this order, all A_i can be expressed in terms of M, κ , G_E , G_M , r_E^2 , $\bar{\alpha}_E$, and $\bar{\beta}_M$.

3. GENERALIZED POLARIZABILITIES

For the purpose of analyzing the model-dependent terms specific to VCS, the invariant amplitude is split into a pole piece \mathcal{M}_A and a residual part \mathcal{M}_B . The s- and u-channel pole diagrams are calculated using electromagnetic vertices of the form

$$\Gamma^{\mu}(p',p) = \gamma^{\mu}F_1(q^2) + i\frac{\sigma^{\mu\nu}q_{\nu}}{2M}F_2(q^2), \ q = p' - p,$$
(4)

where F_1 and F_2 are the Dirac and Pauli form factors, respectively. The corresponding amplitude $\mathcal{M}_A^{\gamma^*\gamma}$ contains all irregular terms as $q \to 0$ or $q' \to 0$ and is separately gauge invariant.

The generalized polarizabilities in VCS [5] result from an analysis of $\mathcal{M}_B^{\gamma^*\gamma}$ in terms of electromagnetic multipoles $H^{(\rho'L',\rho L)S}(\omega',\bar{q})$, where $\rho(\rho')$ denotes the type of the initial (final) photon ($\rho = 0$: charge, C; $\rho = 1$: magnetic, M; $\rho = 2$: electric, E). The initial (final) orbital angular momentum is denoted by L(L'), and S distinguishes between non-spin-flip (S = 0) and spin-flip (S = 1) transitions. According to the LET for VCS, $\mathcal{M}_B^{\gamma^*\gamma}$ is at least linear in the energy of the real photon. A restriction to the lowest-order, i.e. linear terms in ω' leads to only electric and magnetic dipole radiation in the final state. Parity and angular-momentum selection rules (see Table 1) then allow for 3 scalar multipoles (S = 0) and 7 vector multipoles (S = 1). The 10 GPs, $P^{(01,01)0}$, ..., $\hat{P}^{(11,2)1}$, are functions of \bar{q}^2 and are related to the corresponding multipole amplitudes as

$$P^{(\rho'L',\rho L)S}(\bar{q}^2) = \left[\frac{1}{\omega'^L \bar{q}^L} H^{(\rho'L',\rho L)S}(\omega',\bar{q})\right]_{\omega'=0},$$
(5)

$$\hat{P}^{(\rho'L',L)S}(\bar{q}^2) = \left[\frac{1}{\omega'^L \bar{q}^{L+1}} \hat{H}^{(\rho'L',L)S}(\omega',\bar{q})\right]_{\omega'=0},$$
(6)

Table 1Multipolarities of initial and final states

J^P	final real photon	initial virtual photon
$\frac{1}{2}^{-}$	$\mathrm{E1}$	C1,E1
$\frac{3}{2}^{-}$	E1	C1,E1,M2
$\frac{1}{2}^{+}$	M1	C0,M1
$\frac{3}{2}^{+}$	M1	C2,E2,M1

where mixed-type polarizabilities, $\hat{P}^{(\rho'L',L)S}(\bar{q}^2)$, have been introduced which are neither purely electric nor purely Coulomb type (see [5] for details). Only six of the above ten GPs are independent, if charge-conjugation symmetry is imposed [7,8].

4. RESULTS IN CHIRAL PERTURBATION THEORY

The calculation of the generalized polarizabilities is performed within the heavy-baryon formulation of chiral perturbation theory (HBChPT) [10] to third order in the external momenta. At $O(p^3)$, contributions to the GPs are generated by nine one-loop diagrams and the π^0 -exchange *t*-channel pole graph (see [9]). For the loop diagrams only the leading-order Lagrangians are required [10],

$$\widehat{\mathcal{L}}_{\pi N}^{(1)} = \bar{N}_v (iv \cdot D + g_A S \cdot u) N_v, \quad \mathcal{L}_{\pi \pi}^{(2)} = \frac{F_\pi^2}{4} \operatorname{Tr} \left[\nabla_\mu U (\nabla^\mu U)^\dagger \right], \tag{7}$$

where N_v represents a non-relativistic nucleon field, and $U = \exp(i\vec{\tau} \cdot \vec{\pi}/F_{\pi})$ contains the pion field. The covariant derivatives $\nabla_{\mu}U$ and $D_{\mu}N_v$ include the coupling to the electromagnetic field, and u_{μ} contains in addition the derivative coupling of a pion. In the heavy-baryon formulation the spin matrix is given by $S^{\mu} = i\gamma_5\sigma^{\mu\nu}v_{\nu}$, where v^{μ} is a four-vector satisfying $v^2 = 1, v_0 \ge 1$ [10]. Finally, for the π^0 -exchange diagram we require in addition to Eq. (7) the $\pi^0\gamma\gamma^*$ vertex provided by the Wess-Zumino-Witten Lagrangian,

$$\mathcal{L}_{\gamma\gamma\pi^{0}}^{(WZW)} = -\frac{e^{2}}{32\pi^{2}F_{\pi}} \epsilon^{\mu\nu\alpha\beta}F_{\mu\nu}F_{\alpha\beta}\pi^{0}, \qquad (8)$$

where $\epsilon_{0123} = 1$ and $F_{\mu\nu}$ is the electromagnetic field strength tensor.

At $O(p^3)$, the LET of VCS is reproduced by the tree-level diagrams obtained from Eq. (7) and the relevant part of the second- and third-order Lagrangian [12],

$$\widehat{\mathcal{L}}_{\pi N}^{(2)} = -\frac{1}{2M} \bar{N}_v \left[D \cdot D + \frac{e}{2} (\mu_S + \tau_3 \mu_V) \varepsilon_{\mu\nu\rho\sigma} F^{\mu\nu} v^{\rho} S^{\sigma} \right] N_v, \tag{9}$$

$$\widehat{\mathcal{L}}_{\pi N}^{(3)} = \frac{ie\varepsilon_{\mu\nu\rho\sigma}F^{\mu\nu}}{8M^2}\bar{N}_v \left[\mu_S - \frac{1}{2} + \tau_3(\mu_V - \frac{1}{2})\right]S^{\rho}D^{\sigma}N_v + h.c.$$
(10)

The numerical results for the ten generalized proton polarizabilities are shown in Fig. 1 [13]. As an example for S = 0, let us discuss the generalized electric polarizability $\bar{\alpha}_E(\bar{q}^2)$,

$$\frac{\bar{\alpha}_E(\bar{q}^2)}{\bar{\alpha}_E} = 1 - \frac{7}{50} \frac{\bar{q}^2}{m_\pi^2} + \frac{81}{2800} \frac{\bar{q}^4}{m_\pi^4} + O\left(\frac{\bar{q}^6}{m_\pi^6}\right), \ \bar{\alpha}_E = \frac{5e^2 g_A^2}{384\pi^2 m_\pi F_\pi^2} = 12.8 \times 10^{-4} \,\mathrm{fm}^3. \tag{11}$$

For $\bar{q}^2 = 0$, the generalized electric polarizability $\bar{\alpha}_E(\bar{q}^2)$ coincides with the electric polarizability $\bar{\alpha}_E$ of real Compton scattering [5,7]. The prediction of the $O(p^3)$ calculation for $\bar{\alpha}_E(0) =$

 $\bar{\alpha}_E$ agrees well with the experimental value extracted from real Compton scattering, $(12.1 \pm 0.8 \pm 0.5) \times 10^{-4} \text{ fm}^3$ [11]. In ChPT at $O(p^3)$ the generalized electric polarizability decreases considerably faster with \bar{q}^2 than in the constituent quark model [5]. Note that at $O(p^3)$, the results are entirely given in terms of the pion mass m_{π} , the axial coupling constant g_A , and the pion decay constant F_{π} . This feature is true for all generalized polarizabilities.

The π^0 -exchange diagram only contributes to the spin-dependent GPs. As an example for a spin-dependent GP, let us consider $P^{(11,11)1}$,

$$P^{(11,11)1}(\bar{q}^2) = -\frac{1}{288} \frac{g_A^2}{F_\pi^2} \frac{1}{\pi^2 M} \left[\frac{\bar{q}^2}{m_\pi^2} - \frac{1}{10} \frac{\bar{q}^4}{m_\pi^4} \right] + \frac{1}{3M} \frac{g_A}{8\pi^2 F_\pi^2} \tau_3 \left[\frac{\bar{q}^2}{m_\pi^2} - \frac{\bar{q}^4}{m_\pi^4} \right] + O\left(\frac{\bar{q}^6}{m_\pi^6}\right).$$
(12)

As a consequence of C invariance, $P^{(11,11)1}(0) = 0$ [8] which, e.g., is not true for the constituent quark model [5]. The predictions for the spin-dependent GPs originate from two rather distinct sources—an isoscalar piece from pionic loop contributions, and an isovector piece from the $\pi^0 \gamma \gamma^*$ vertex. It is interesting that the contributions of the pion-nucleon loops to the spin-dependent GPs are much smaller than the contributions arising from the π^0 -exchange diagram.

REFERENCES

- 1. F.E. Low, Phys. Rev. 96 (1954) 1428.
- 2. M. Gell-Mann and M.L. Goldberger, Phys. Rev. 96 (1954) 1433.
- 3. B.R. Holstein, Comments Nucl. Part. Phys. 20 (1992) 301.
- G. Audit *et al.*, CEBAF Report No. PR 93-050 (1993); J.F.J. van den Brand *et al.*, CEBAF Report No. PR 94-011 (1994); G. Audit *et al.*, MAMI proposal "Nucleon structure study by Virtual Compton Scattering." (1995); J. Shaw *et al.*, MIT-Bates proposal No. 97-03 (1997).
- 5. P.A.M. Guichon, G.Q. Liu, A.W. Thomas, Nucl. Phys. A591 (1995) 606.
- 6. S. Scherer, A.Yu. Korchin, J.H. Koch, Phys. Rev. C54 (1996) 904.
- 7. D. Drechsel, G. Knöchlein, A. Metz, S. Scherer, Phys. Rev. C55 (1997) 424.
- 8. D. Drechsel, G. Knöchlein, A.Yu. Korchin, A. Metz, S. Scherer, nucl-th/9704064.
- 9. T.R. Hemmert, B.R. Holstein, G. Knöchlein, S. Scherer, Phys. Rev. D55 (1997) 2630.
- E. Jenkins and A. Manohar, Phys. Lett. B255 (1991) 558; V. Bernard, N. Kaiser, J. Kambor, U.-G. Meißner, Nucl. Phys. B388 (1992) 315.
- 11. B.E. MacGibbon et al., Phys. Rev. C52 (1995) 2097.
- 12. G. Ecker and M. Mojžiš, Phys. Lett. B365 (1996) 312.
- 13. T.R. Hemmert, B.R. Holstein, G. Knöchlein, S. Scherer, Phys. Rev. Lett. 79 (1997) 22.

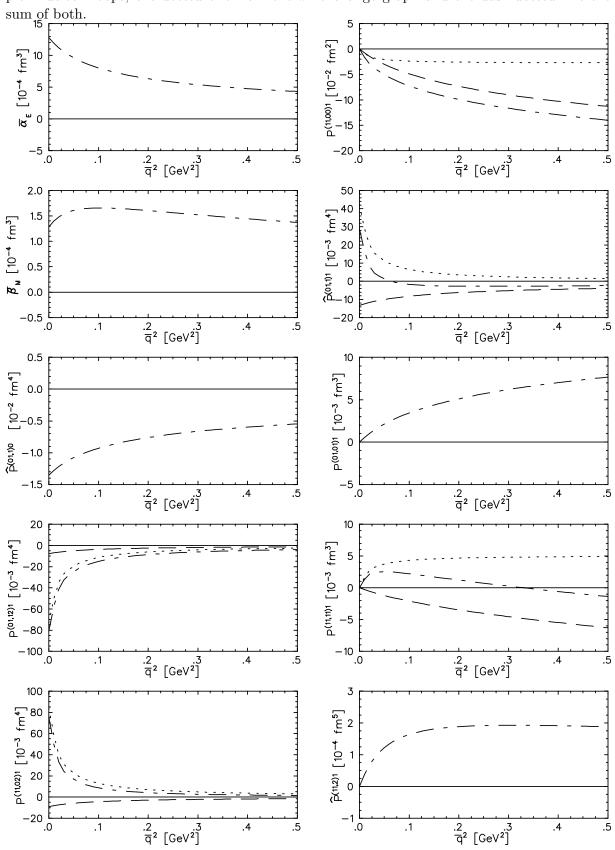


Figure 1. GPs of the proton as a function of \bar{q}^2 . The dashed line is the contribution from pion-nucleon loops, the dotted one from the π^0 exchange graph and the dash-dotted line the sum of both.